

## Development and characterization of hybrid thin-ply composite materials

Argyropoulos, Alexios ; Caglar, Baris; Gomasasca, S.; Ricard, Thomas ; Michaud, Véronique

**Publication date**

2022

**Document Version**

Final published version

**Published in**

Proceedings of the 20th European Conference on Composite Materials: Composites Meet Sustainability

**Citation (APA)**

Argyropoulos, A., Caglar, B., Gomasasca, S., Ricard, T., & Michaud, V. (2022). Development and characterization of hybrid thin-ply composite materials. In A. P. Vassilopoulos, & V. Michaud (Eds.), *Proceedings of the 20th European Conference on Composite Materials: Composites Meet Sustainability: Vol 1 – Materials* (pp. 1236-1243). EPFL Lausanne, Composite Construction Laboratory.

**Important note**

To cite this publication, please use the final published version (if applicable).  
Please check the document version above.

**Copyright**

Other than for strictly personal use, it is not permitted to download, forward or distribute the text or part of it, without the consent of the author(s) and/or copyright holder(s), unless the work is under an open content license such as Creative Commons.

**Takedown policy**

Please contact us and provide details if you believe this document breaches copyrights.  
We will remove access to the work immediately and investigate your claim.

## DEVELOPMENT AND CHARACTERIZATION OF HYBRID THIN-PLY COMPOSITE MATERIALS

Alexios Argyropoulos<sup>a,c</sup>, Baris Caglar<sup>b</sup>, Silvia Gomasasca<sup>b</sup>, Thomas Ricard<sup>c</sup>, Veronique Michaud<sup>a</sup>

a: Laboratory for Processing of Advanced Composites (LPAC), Institute of Materials (IMX), Ecole Polytechnique Fédérale de Lausanne (EPFL), Station 12, Lausanne, CH-1015, Switzerland – [alexios.argyropoulos@epfl.ch](mailto:alexios.argyropoulos@epfl.ch)

b: Aerospace Manufacturing Technologies, Faculty of Aerospace Engineering, Delft University of Technology, Kluyverweg 1, Delft 2629HS, The Netherlands

c: North Thin Ply Technology SARL, Chemin du Closel 3, 1020 Renens, Switzerland

**Abstract:** *The mechanical shaping process of calendering was employed for the manufacturing of hybrid pre-impregnated tapes of reduced thickness (thin-ply prepregs) by comingling various ratios of dissimilar carbon fibres with different processing parameters. A versatile image processing and microstructural analysis tool was developed to capture the arrangement of the different fibres in cross-sections of multi-layer laminates produced with the calendered materials. The performance of the calendering process as a method of manufacturing hybrid thin-ply prepregs was evaluated through the degree of hybridization that could be achieved and the effect of processing parameters on the overall microstructure of the hybrids.*

**Keywords:** hybrid composites; thin-ply; microstructural characterization

### 1. Introduction

Thin-ply composites are recognized as a key solution for the manufacturing of high-performance composite structures due to the unique mechanical properties and the increased design versatility that they offer. However, the high production cost due to the complexity of the manufacturing methods and their inherent brittleness limit their wider adoption by the composites industry [1]. In recent years, fibre hybridization (i.e., combining at least two types of fibres in a common matrix) is emerging as a promising approach for alleviating these drawbacks towards laminates with balanced characteristics in terms of mechanical properties and cost-efficiency [2]. Currently, most studies on hybrids employ simple interlayer (ply-level) configurations mainly due to difficulties in manufacturing more complex tow or fiber-level architectures[3]. However, simulation tools predict that notable improvements can be obtained from hybrids with an increased level of fiber dispersion [4]. The main aim of this work is to experimentally evaluate the efficiency of the calendering process as a new methodology for manufacturing prepregs that combine thin-ply and hybrid characteristics.

### 2. Materials and Methods

#### 2.1 Materials

Two different grades of continuous tows of carbon fibres were selected for the present study. The high strain GRAFIL™ 34-700WD (HS:  $E_f=234$  GPa,  $\epsilon_f=2.06\%$ ) and the low strain PYROFIL™ HR 40 12M (LS:  $E_f=375$  GPa  $\epsilon_f=1.18\%$ ) both produced by Mitsubishi. The matrix was ThinPreg™ 415 (TP415), a rubber toughened epoxy formulation of North Thin Ply Technology (NTPT). The materials were processed by NTPT to produce single-fiber unidirectional (UD) thin-ply prepregs

with different ply fiber areal weight (FAW), that were used as an intermediate stage of hybrid prepreg manufacturing. Rolls with FAW of 30g/m<sup>2</sup> (gsm) and 60 gsm were manufactured with the 34-700 fibres and an ultra-thin ply format with FAW of 15 gsm was chosen for the HR40 fibres. The nominal resin content (RC) for all prepregs was set at 37% by weight.

## 2.2 Manufacturing of hybrid prepregs with the calendering process

A custom-made calender consisting of two heated counter-rotating steel rolls, schematically presented in Figure 1, was assembled for manufacturing the hybrid prepregs. Key production settings of the calender apparatus such as the rotational speed, the temperature, and more importantly the distance between the rolls that controlled the applied pressure on the unidirectional prepregs, could be accurately adjusted during production, securing a smooth and uninterrupted operation. To produce prepregs with an increased level of fibre co-dispersion and ideally fibre level hybrids, pairs of different single-fiber UD thin-ply prepregs manufactured at previous stages were aligned on top of each other and then guided in the tight nip created between the calender rolls at elevated temperatures. The pressure of the rolls forced the dissimilar fibres of the prepregs to interpenetrate and create fibre-level hybrid configurations. In total, four different calendered and two baseline non-calendered equivalent hybrid thin-ply prepregs were manufactured for this work, as described in *Table 1*. Hybrid composite laminates were manufactured with each material type by manually stacking hybrid plies on top of each other and the number of them was adjusted to reach a thickness of 2mm. The laminates were then cured in an autoclave following the curing profile recommended by NTPT (125°C, 2h, 5atm peak pressure) to fully cross-link the TP415 epoxy matrix and reach optimal performance for the hybrid thin-ply composite.

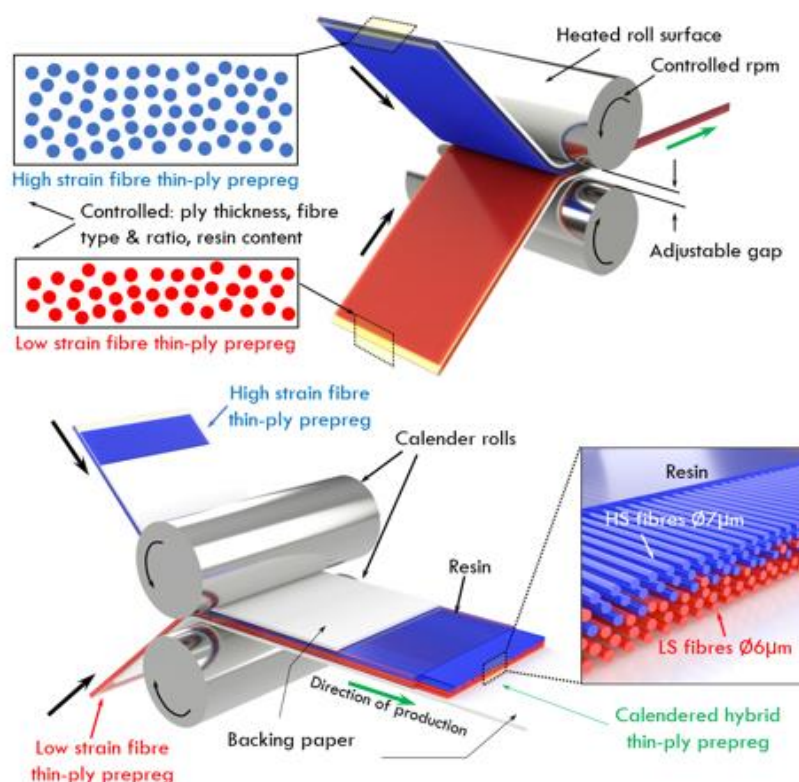


Figure 1 Schematic of the calendering process and calender apparatus employed for the manufacturing of hybrid thin-ply prepregs.

**Table 1** Production characteristics and fibre composition of hybrid thin-ply preregs

Calender Pressure	Low Strain Fibre (LS) HR40 (g/m <sup>2</sup> )	High Strain Fibre (HS) 34-700 (g/m <sup>2</sup> )	Hybrid FAW (g/m <sup>2</sup> )	Sample Reference
Low	15	60	75	C LP 75
Low	15	30	45	C LP 45
High	15	60	75	C HP 75
High	15	30	45	C HP 45
Non-Calendered	15	60	75	NC 75
Non-Calendered	15	30	45	NC 45

### 2.3 Microstructural characterization of hybrid thin-ply composite laminates

Microstructural analysis techniques were used to quantify the effect of processing parameters on the overall microstructural profile of hybrid composites produced with calendered thin-ply preregs. Cross-sections of the multilayer hybrid laminates were embedded into resin blocks that were ground with SIC abrasive papers (grain size P:400 - P:1200) and then polished for long cycles on a cloth pad with diamond abrasive suspension (particle size 1-3  $\mu\text{m}$ ) to obtain mirror-finished surfaces. These micrography samples were observed with a KEYENCE VHX-600 optical digital microscope under lighting conditions that could best produce high contrast between the matrix and the different reinforcements since the quality of the raw images can strongly affect the results of fibre identification and image analysis methods. The workflow for the identification of fibre position and type is shown in *Figure 2*. Matrix and fibres were segmented from the raw image in Fiji [5] via Minimum threshold. The following steps were conducted in Matlab. A morphological operation of opening was used to reduce thresholding artefacts prior to fibre identification via Circular Hough Transform. Analysis of the gradient magnitude on the location of each fibre was conducted on the raw image, leading to a bimodal distribution in which peaks correspond to each fibre type.

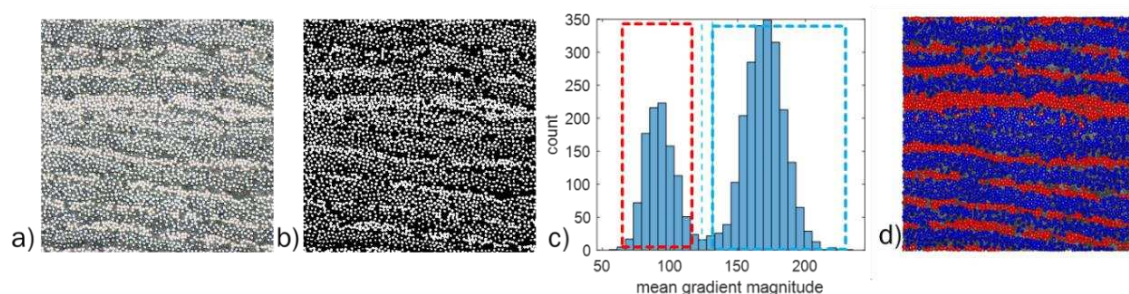


**Figure 2** Workflow for fibre type identification: a) raw image b) image after thresholding and morphological operations c) histogram of the mean local gradient magnitude, showing a bimodal distribution where the two peaks can be associated to each fibre type (left: HR40 (low strain, LS); right: 34-700 (high strain, HS)) d) resulting fibre type assignment based on the bimodal distribution.

### 2.3.1 Hybrid parameters calculation

The metrics were based on the parameters of areal disorder [6], dispersion [2], and degree of hybridization [7]. To investigate the variability of the metrics for each material, the parameters were evaluated in three different regions of area 1600  $\mu\text{m}$  by 1300  $\mu\text{m}$ . Nominal fibre diameters were used for the calculations (7  $\mu\text{m}$  for high strain (HS) fibres [8] and 6  $\mu\text{m}$  for low strain (LS) fibres).

#### 2.2.1 Areal disorder

The areal disorder (AD) was determined using a Delaunay tessellation as defined by Bray et al.[6]:

$$AD = \left( \frac{A}{\sigma} + 1 \right)^{-1}, \quad (1)$$

where A is the mean area of the elements in the tessellation and  $\sigma$  is the corresponding standard deviation. In this work, AD was calculated for each sample on three different tessellations, one which considers globally all fibre centres and one considering LS fibres only and a third one considering HS fibres only.

#### 2.2.2 Dispersion

In literature, the dispersion parameter was used to quantify the degree of fibre mixing by considering the proximity of two different fibre types  $F_A$  and  $F_B$ :

$$\text{Dispersion} = \text{mean} \left( \frac{R_{F_A}}{\sum_{i=1 \dots 6} d(F_{A_j} \rightarrow F_{B_i}) / 6} \right) \text{ all } j \quad (2)$$

where  $R_{F_A}$  is the nominal radius of fibre type  $F_A$ ,  $d(F_{A_j} \rightarrow F_{B_i})$  is the distance between the  $j$ -th fibre of type  $F_A$  and the six closest neighbouring fibres of type  $F_B$ . To understand the ability of the parameter to capture effects in an anisotropic fibre arrangement such as those encountered in this study, the parameter was calculated with reference to both low strain (LS) and high strain (HS) fibres, compared to only on low strain (LS) fibres as reported in the literature[2].

#### 2.2.3 Degree of hybridization

The degree of hybridization compares the local fibre composition of a given microstructure to that of a microstructure with random fibre distribution [7]. A square moving window was used to determine the local areal ratio (AR) of the two fibre types over the region analysed, as:

$$AR = \frac{N_{F_A} D_{F_A}^2}{(N_{F_A} D_{F_A}^2 + N_{F_B} D_{F_B}^2)} \quad (3)$$

where  $N_{F_A}$  and  $N_{F_B}$  are the number of fibres of the two types, and  $D_{F_A}$  and  $D_{F_B}$  the corresponding nominal diameters. The window size was chosen equal to six times the nominal diameter as suggested in the literature [7] and was determined as the weighted ratio of the nominal values of the fibres diameters in the mean fibre composition for the dataset. The degree of hybridization (H) was then defined as the ratio between the coefficient of variation of the areal ratio distribution of each sample and that of a random hybrid microstructure, expressed as a percentage. For this analysis, the random microstructure was chosen to have same fibre type ratio, fibre number and positions as in each sample, but with a random fibre assignment.

### 3. Results and discussion

The samples show a range of volume fractions as shown in *Figure 3*. The resulting general trend shows an increase in global fibre volume fraction with increasing calendaring pressure. Additional effects arising from debulking cycles are not investigated.

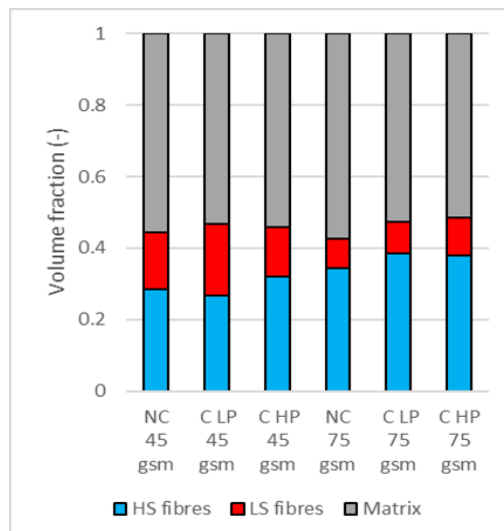


*Figure 3 Laminate compositions expressed as volume fraction of the individual components.*

#### 3.1 Areal disorder

The results of the analysis of the areal disorder (AD) are reported in *Figure 4a*. The values of AD for the global fibre distributions are similar for all samples and lower than the values determined for either LS and HS fibre types taken individually. A higher value of global AD is observed for the non-calendered (NC) samples compared to calendered (C) samples. An increase in the value of AD for the LS fibres (in red) is observed for both increasing calendaring pressure and for increasing nominal areal weight of HS fibres. For the HS fibres (in blue), the value of AD has a lower range of variation between samples compared to that for the LS fibres. A lower value of areal disorder corresponds to a more regular fibre distribution. For this reason, the AD for the global fibre architecture is always lower than for the individual phases, which have a greater variation in tessellation area due to the presence of alternated regions of higher packing density (within each individual layer), and empty regions occupied by the other fibre type. A slightly higher value of global AD is observed for non-calendered (NC) samples compared to calendered (C) samples, which might indicate a higher level of overall disorder in the material. Since the increase in HS fibres nominal areal weight from 30 gsm to 60 gsm translates into a greater spacing between layers of LS fibres, the latter phase appears overall less ordered, resulting in an increase in AD. For the HS fibres, the variability between samples can be appreciated less over this range of compositions.

#### 3.2 Dispersion

As shown in *Figure 4b*, little variation in dispersion is observed between different samples for LS fibres (in red). Conversely, a general decrease of dispersion for HS fibres (in blue) is observed with the increase of the nominal HS fibre areal weight from 30 g/m<sup>2</sup> (gsm) to 60 g/m<sup>2</sup>.



Since the areal weight of the LS fibre layer is similar for all samples, the resulting layer thickness is similar in all samples. For this reason, the distance to the six closest neighbours of the opposite fibre type varies only slightly between samples, leading to small changes in the values of dispersion. Conversely, for an increase in nominal HS fibres areal weight, the average distance to the six closest LS fibres will increase. This might have a different effect depending on the effective HS fibre fraction shown in *Figure 3*, which might determine a variation in the average layer thickness.

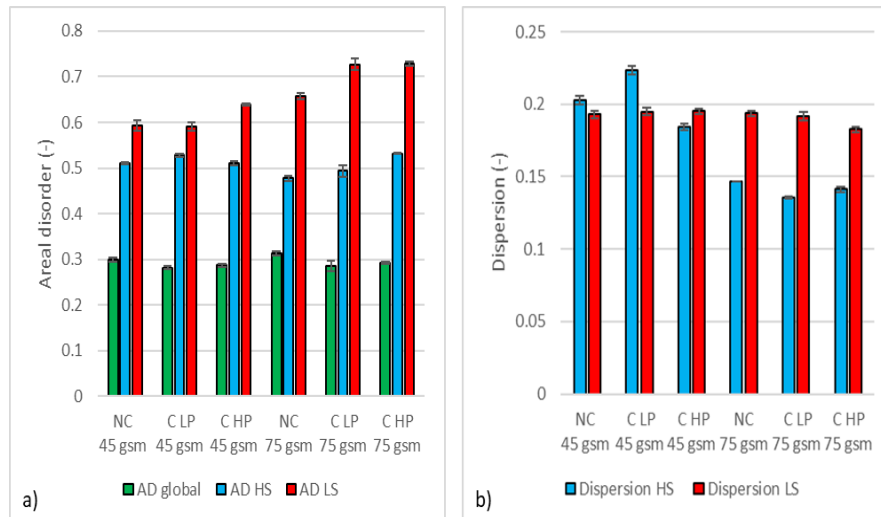


*Figure 4 a) Areal disorder for the two fibre types (HS in blue and LS in red) and for the global fibre arrangement (in green) b) Dispersion for the two fibre types (HS in blue and LS in red).*

### 3.3 Degree of hybridization

The distribution of areal ratios for each sample and for their corresponding random microstructures are shown in *Figure 4a*. A higher number of regions containing only HS fibres is present for increasing HS fibre nominal areal weight, which is shown by a higher bin count at AR=1. The resulting degree of hybridization shown in *Figure 4b* decreases with increasing HS fibre nominal areal weight and is highest for the non-calendered samples within each nominal composition. The degree of hybridization was calculated with reference to HS fibres. Choosing to refer to LS fibres instead would have led to a flipped distribution of areal disorder values, and therefore would not have affected the current analysis. A window size equal to six times the nominal fibre diameter was chosen as recommended in the literature [7], however, a different choice of size is expected to impact the result, as the greater the window size, the greater the microstructural homogenization in the resulting AR distribution. The choice of random microstructures tailored to each sample to match their fibre type composition was considered necessary to generate comparable datasets, due to the variations in fibre type composition shown in *Figure 3*. The greater degree of hybridization for the LS 15 gsm – HS 30 gsm sample series relates to a more homogenous microstructure within the window of observation chosen compared to the LS 15 gsm – HS 60 gsm series due to lower spacing between different layer types. Within each sample series, a greater degree of hybridization is observed for non-calendered samples compared to the calendered counterparts.

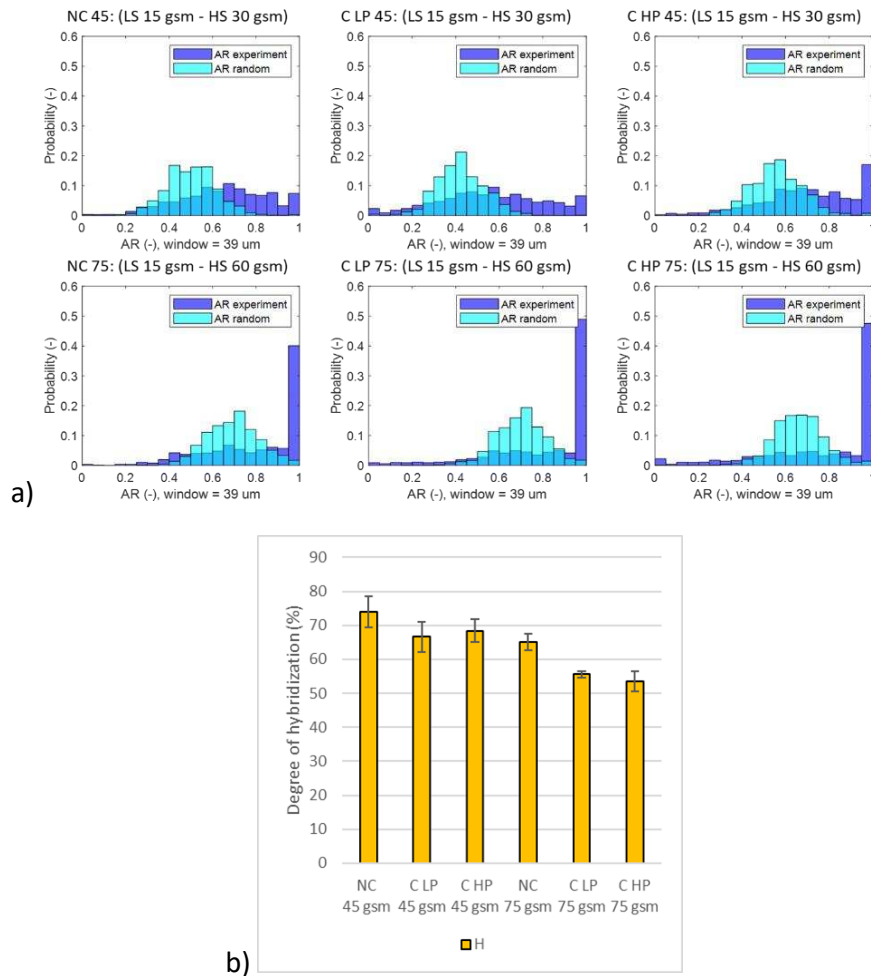


Figure 5 a) Distributions of areal ratio (AR) for the four samples b) resulting degree of hybridization (H)

#### 4. Conclusions

Unidirectional hybrid pre-impregnated tapes were successfully manufactured via the newly developed calendering process by comingling various ratios of low strain (LS) and high strain (HS) carbon fibres under different processing conditions. Optical microscopy was used to reveal the microstructural features of cured multi-layer composite laminates manufactured with the calendered hybrid prepreps and a fiber identification and microstructural analysis tool was developed for the characterization of the new materials. Three parameters were used to describe the hybrid microstructure: areal disorder [6], dispersion [2] and degree of hybridization [7]. All parameters were able to capture differences between samples which are linked to size effects related to varying layer thickness. Calendering effects were mostly captured by areal disorder and degree of hybridization. Lower areal disorder in LS fibres and greater degree of hybridization were encountered for non-calendered samples compared to the high-pressure calendered counterpart, suggesting greater local fibre intermingling for the former.



## Acknowledgments

The research leading to these results has been performed within the framework of the HyFiSyn project and has received funding from the European Union's Horizon 2020 research and innovation programme under the Marie Skłodowska-Curie grant agreement No 765881.

## 5. References

- [1] J. Cugnoni *et al.*, "Towards aerospace grade thin-ply composites: Effect of ply thickness, fibre, matrix and interlayer toughening on strength and damage tolerance," *Compos. Sci. Technol.*, vol. 168, pp. 467–477, Nov. 2018, doi: 10.1016/j.compscitech.2018.08.037.
- [2] Y. Swolfs, I. Verpoest, and L. Gorbatikh, "Recent advances in fibre-hybrid composites: materials selection, opportunities and applications," *Int. Mater. Rev.*, vol. 64, no. 4, pp. 181–215, May 2019, doi: 10.1080/09506608.2018.1467365.
- [3] G. Czél, M. Jalalvand, and M. R. Wisnom, "Design and characterisation of advanced pseudo-ductile unidirectional thin-ply carbon/epoxy–glass/epoxy hybrid composites," *Compos. Struct.*, vol. 143, pp. 362–370, May 2016, doi: 10.1016/j.compstruct.2016.02.010.
- [4] Y. Swolfs, R. M. McMeeking, I. Verpoest, and L. Gorbatikh, "The effect of fibre dispersion on initial failure strain and cluster development in unidirectional carbon/glass hybrid composites," *Compos. Part Appl. Sci. Manuf.*, vol. 69, pp. 279–287, Feb. 2015, doi: 10.1016/j.compositesa.2014.12.001.
- [5] J. Schindelin *et al.*, "Fiji: an open-source platform for biological-image analysis," *Nat. Methods*, vol. 9, no. 7, pp. 676–682, Jun. 2012, doi: 10.1038/nmeth.2019.
- [6] D. J. Bray, S. G. Gilmour, F. J. Guild, and A. C. Taylor, "The effects of particle morphology on the analysis of discrete particle dispersion using Delaunay tessellation," *Compos. Part Appl. Sci. Manuf.*, vol. 54, pp. 37–45, Nov. 2013, doi: 10.1016/j.compositesa.2013.07.003.
- [7] H. Diao, A. Bismarck, P. Robinson, and M. R. Wisnom, "Production of continuous intermingled CF/GF hybrid composite via fibre tow spreading technology," *16th Eur. Conf. Compos. Mater. ECCM 2014*, Jan. 2014.
- [8] F. Mesquita, Y. Swolfs, S. Bucknell, Y. Leray, S. V. Lomov, and L. Gorbatikh, "TENSILE PROPERTIES OF SINGLE CARBON FIBRES TESTED WITH AUTOMATED EQUIPMENT," p. 7.